Calcium Activates Erythrocyte AMP Deaminase [Isoform E (AMPD3)] through a Protein−Protein Interaction between Calmodulin and the N-Terminal Domain of the AMPD3 Polypeptide†

Donna K. Mahnke and Richard L. Sabina*

Department of Biochemistry, Medical College of Wisconsin, Milwaukee, Wisconsin 53226

Received August 31, 2004; Revised Manuscript Received January 25, 2005

ABSTRACT: Erythrocyte AMP deaminase [isoform E (AMPD3)] is activated in response to increased intracellular calcium levels in Tarui's disease, following exposure of ionophore-treated cells to extracellular calcium, and by the addition of calcium to freshly prepared hemolysates. However, the assumption that Ca^{2+} is a positive effector of isoform E is inconsistent with the loss of sensitivity to this divalent cation following dilution of erythrocyte lysates or enzyme purification. Ca^{2+} regulation of isoform E was studied by examining in vitro effects of calmodulin (CaM) on this enzyme and by monitoring the influence of CaM antagonists on purine catabolic flow in freshly prepared erythrocytes under various conditions of energy imbalance. Erythrocyte and recombinant isoform E both adsorb to immobilized Ca^{2+}-CaM, and relative adsorption across a series of N-truncated recombinant enzymes localizes CaM binding determinants to within residues 65−89 of the AMPD3 polypeptide. Ca^{2+}-CaM directly stimulates isoform E catalytic activity through a K_{mapp} effect and also antagonizes the protein−lipid interaction between this enzyme and intracellular membranes that inhibits catalytic activity. AMP is the predominant purine catabolite in erythrocytes deprived of glucose or exposed to A23187 ionophore alone, whereas IMP accumulates when Ca^{2+} is included under the latter conditions and also during autoincubation at 37 °C. Preincubation with a CaM antagonist significantly slows the accumulation of erythrocyte IMP under both conditions. The combined results reveal a protein−protein interaction between Ca^{2+}-CaM and isoform E and identify a mechanism that advances our understanding of erythrocyte purine metabolism. Ca^{2+}-CaM overcomes potent isoform E inhibitory mechanisms that function to maintain the total adenine nucleotide pool in mature erythrocytes, which are unable to synthesize AMP from IMP because of a developmental loss of adenylosuccinate synthetase. This may also explain why Tarui's disease erythrocytes exhibit accelerated adenine nucleotide depletion in response to an increase in intracellular Ca^{2+} concentration. This regulatory mechanism could also play an important role in purine metabolism in other human tissues and cells where the AMPD3 gene is expressed.

AMP deaminase (AMPD)[1] is a highly regulated tetrameric enzyme that catalyzes a branch point reaction in the ATP catabolic pathway. AMPD competes with AMP-preferring cytosolic 5′-nucleotidase (cNT-I) for available substrate, and regulation of these two enzymes determines the metabolic fate of AMP during periods of energy imbalance. cNT-I dephosphorylates AMP and produces adenosine, a diffusible compound with pleiotropic intracellular and extracellular effects (*1*−*3*). Alternatively, AMPD deaminates AMP to IMP and retains the purine ring structure at the nucleotide level. IMP may then be funneled into a branch of the ATP catabolic pathway that bypasses adenosine, diverted into the guanine nucleotide pool, or converted back to AMP. Mammalian species, including humans, contain three AMPD genes that exhibit tissue-specific and developmental patterns of expression (*4*−*6*). Each human AMPD gene contains coding information for an isoform named after the source of initial purification: AMPD1, isoform M (muscle); AMPD2, isoform L (liver); and AMPD3, isoform E (erythrocyte). AMPD1 expression is restricted primarily to postnatal skeletal muscle, whereas the other two genes are widely expressed. Alignments reveal conserved C-terminal and divergent N-terminal primary amino acid sequence in each human AMPD polypeptide (*7*, *8*), and a growing body of evidence indicates that these variable domains are involved in isoform-specific behaviors of the enzyme (*9*−*12*).

Situations in which AMPD expression is altered can provide insight into the functional significance of this enzymatic activity in human tissues and cells. This is perhaps best illustrated in mature erythrocytes, which are unable to

† This work was supported by U.S. Public Health Service Grant DK-50902 from the National Institutes of Health and by a grant from the Medical College of Wisconsin Research Affairs Committee.

* To whom correspondence should be addressed: Department of Biochemistry, 8701 Watertown Plank Rd., Milwaukee, WI 53226. Phone: (414) 456-4697. Fax: (414) 456-6510. E-mail: sabinar@mcw.edu.

[1] Abbreviations: AMPD, AMP deaminase; CaM, calmodulin; cNT-I, cytosolic 5′-nucleotidase; PtdIns(4,5)P2, phosphatidylinositol 4,5-bisphosphate; W13, *N*-(4-aminobutyl)-5-chloro-2-naphthalenesulfonamide; W12, *N*-(4-aminobutyl)-2-naphthalenesulfonamide; W7, *N*-(6-aminohexyl)-5-chloro-1-naphthalenesulfonamide; Sf9, *Spodoptera frugiperda*; EGTA, ethylene glycol bis(β-aminoethyl ether)-*N*,*N*,*N*′,*N*′-tetraacetic acid; 5P8, 5 mM sodium phosphate at pH 8.0; EG, unsealed erythrocyte ghosts; BSA, bovine serum albumin.

10.1021/bi048121p CCC: $30.25
Published on Web 03/18/2005

synthesize AMP from IMP because of a developmental loss of adenylosuccinate synthetase (*13*, *14*). Consequently, AMP deamination irreversibly depletes the erythrocyte adenine nucleotide pool, and isoform E catalytic activity must be tightly regulated to maintain steady-state ATP levels. Oxidative stress (*15*, *16*) and a disturbed calcium homeostasis in familial phosphofructokinase deficiency (Tarui's disease) (*17*) are situations in which increased erythrocyte AMPD activity is observed and are both accompanied by accelerated adenine nucleotide depletion and higher rates of hemolysis. Conversely, an inherited AMPD3 deficiency in the Japanese (*18*, *19*) and Caucasian (*20*) populations is asymptomatic and characterized by elevated levels of erythrocyte ATP.

Chemical modifiers of sulfhydryl groups reportedly mimic the effect of oxidative stress on erythrocyte AMPD (*16*). Alternatively, Ca^{2+} has been proposed as an activator of AMPD in Tarui's disease erythrocytes (*17*), and observations made in normal cells appear to support this hypothesis. For example, there is a dramatic accumulation of IMP when intact erythrocytes are simultaneously exposed to the A23187 ionophore and $CaCl_2$ (*21*, *22*). In addition, initial rates of AMP deamination in freshly prepared hemolysates are 10-fold higher in the presence of saturating Ca^{2+} concentrations (*16*, *21*, *23*). However, this effect is only indirect as evidenced by the loss of calcium sensitivity following dilution of the lysate (*23*) or partial purification of the enzyme (*23*, *24*). These combined observations have led to a proposal for an endogenous AMPD inhibitor in erythrocytes that is weakened in its action by dilution or lost during purification (*23*). The role of calcium in this scheme is envisioned as an antagonist of the inhibitor.

There is a growing body of evidence that suggests the catalytic activity and distribution of isoform E are affected by intracellular protein−lipid interactions, which may represent an important regulatory mechanism for adenine nucleotide branch point catabolism in human tissues and cells that express the AMPD3 gene. AMPD activity is present in human erythrocyte membrane preparations (*24*) and detergent insoluble fractions of adult rat and post-mortem human brain (*10*, *25*), and the latter contain a polypeptide that reacts with anti-AMPD3 serum. In addition, catalytic inhibition and altered secondary structure accompany the binding of purified pig heart AMPD, the porcine ortholog of human isoform E (*26*), to isolated cytoplasmic membrane vesicles and artificial lipid bilayers (*27*−*29*). Purified human erythrocyte AMPD also exhibits lower catalytic activity when bound to unsealed ghost membranes (*30*). Unfortunately, AMPD polypeptides are extremely sensitive to limited proteolysis during purification and subsequent storage of the enzyme (*31*−*34*). Consequently, these previous studies were likely conducted with proteolyzed enzymes, as suggested by available Western blot data (*10*, *25*). However, recent studies conducted with a recombinant enzyme comprised of full-sized subunits have shown that isoform E binds specifically to mixed lipid micelles that contain phosphatidylinositol 4,5-bisphosphate (PtdIns[4,5]P2), which is also a potent noncompetitive inhibitor of catalytic activity (*10*). Recombinant isoform E also binds reversibly to unsealed erythrocyte ghost membranes with associated catalytic inhibition, and this protein−lipid interaction, unlike that of an N-truncated recombinant model of the proteolyzed endogenous enzyme, is sensitive to physiological changes in pH (*12*).

Calmodulin (CaM) is a small, ubiquitous, highly conserved protein that modulates many calcium-dependent processes (see ref *35* for a recent review). CaM is expressed in all eukaryotic cells and participates in signaling pathways that regulate processes such as growth, proliferation, and movement. The biological activity of CaM appears to be related to location and concentration, which can constitute at least 0.1% of the total protein in cells. In human erythrocytes, CaM concentrations have been estimated to be 2.5 ± 0.2 μM (*36*). Included among CaM's many intracellular effects has also been the antagonization of the membrane association of several proteins (*37*−*39*).

These combined features of isoform E and CaM suggest that an interaction between the two proteins could be responsible for the Ca^{2+}-induced activation of erythrocyte AMPD. Most human tissues and cells that contain detectable AMPD3 mRNA also express other members of the multigene family (*5*−*8*) and contain mostly heterotetrameric AMPD enzymes (*40*, *41*). Conversely, erythrocytes produce only isoform E (*41*), which makes them ideally suited as a model system in which to conduct an evaluation of the proposed protein−protein interaction with CaM.

EXPERIMENTAL PROCEDURES

Materials. Grace's insect cell medium and fetal calf serum were purchased from Gibco-BRL. Phosphocellulose (P11) was obtained from Whatman, Ltd. Phenyl Sepharose CL-4B and DEAE Sephacel were supplied by Amersham Phamacia Biotech. Disposable glass columns and a protein assay kit were available through Bio-Rad. Goat anti-rabbit IgG was obtained from Santa Cruz Biotechnology, Inc. Fresh frozen adult bovine brains (stripped) were available from Pel-Freez. Calmodulin−agarose (bovine brain phosphodiesterase 3′,5′-cyclic nucleotide activator−agarose), the A23187 ionophore, and the calmodulin antagonists, *N*-(4-aminobutyl)-5-chloro-2-naphthalenesulfonamide (W13), *N*-(4-aminobutyl)-2-naphthalenesulfonamide (W12), and compound 48/80, were purchased from Sigma. The Blood Center of Southeastern Wisconsin provided outdated packed human erythrocytes. Fresh blood samples were obtained from a control volunteer (R. L. Sabina). All other chemicals and reagents were of the highest commercially available quality.

Expression and Purification of AMPD3 Recombinant Enzymes. Human AMPD3 recombinant enzymes were expressed in Sf9 (*Spodoptera frugiperda*) insect cells using baculoviral technology and purified by phosphocellulose chromatography (sequential potassium chloride and potassium phosphate gradient elution) and ammonium sulfate precipitation as previously described (*9*, *11*, *12*).

Partial Purification of Erythrocyte AMPD. Isoform E was partially purified from outdated human erythrocytes after the method of Nathans et al. (*42*), with some modifications. Briefly, hemolysate was prepared from 250 mL of packed erythrocytes by stirring for 1 h at 4 °C following a 1:1 dilution with ice-cold deionized water containing 30 μg/mL leupeptin. The hemolysate was clarified by centrifugation at 10000*g* for 15 min at 4 °C, batch adsorbed for 1 h at 4 °C with stirring to DEAE that was prepared in potassium phosphate, and equilibrated in deionized water. Adsorbed resin was collected at 4 °C in a Buchner funnel on Whatman 1 filter paper and washed extensively with ice-cold 20 mM

imidazole (pH 7.45) containing 20 mM potassium chloride until the filtrate was clear. Resin was then resuspended in fresh wash buffer, poured into a 3 cm × 13 cm glass column, and allowed to settle overnight at 4 °C. The protein was eluted with 20 mM imidazole (pH 7.0) containing 500 mM potassium chloride and 5 μg/mL leupeptin. The column eluate was monitored with an enzyme assay, and active fractions were pooled and further purified as described above for AMPD3 recombinant proteins. This entire process resulted in 15000-fold purification at 19% recovery and produced a partially purified enzyme with a specific activity of 105 units/mg of protein.

Purification of Bovine Brain Calmodulin. Calmodulin was purified from fresh frozen bovine brain by Phenyl Sepharose chromatography according to a published protocol (*43*) and subsequently rendered free of calcium by being treated with 1 mM ethylene glycol bis(β-aminoethyl ether)-*N*,*N*,*N*′,*N*′-tetraacetic acid (EGTA) followed by extensive dialysis against deionized water.

Adsorption of AMPD Enzymes to Calmodulin−Agarose Beads. One or two units of AMPD3 recombinant enzymes, one unit of partially purified erythrocyte isoform E, or 50 μL of clarified fresh human erythrocyte hemolysate was mixed with 25 μL of calmodulin−agarose beads (50% slurry) equilibrated in 5 mM potassium phosphate (pH 6.6), 45 mM potassium chloride, 0.1% bovine serum albumin (BSA), 10 μg/mL leupeptin, and either 200 μM calcium chloride ($CaCl_2$) or 1 mM EGTA. Mixtures were incubated on ice for 90 min with rotation, and then centrifuged at 14000*g* for 2 min at 4 °C. The supernatants were removed, and the beads were washed several times in the appropriate equilibration buffer ($CaCl_2$ or EGTA) without BSA. Residual AMPD activities were assayed in supernatants, and enzyme partitioning was visualized by 9% SDS−PAGE of supernatant and pellet fractions. The agarose-bound enzyme was eluted from the resin during boiling in sample buffer prior to gel loading.

Effects of Glucose Deprivation and Ionophore on Erythrocyte Nucleotide Pools. Erythrocytes were prepared from fresh whole blood by washing the blood twice in 1 mM sodium phosphate (pH 7.4) containing 150 mM sodium chloride (1P7.4), and then resuspended at a 23% hematocrit in 1P7.4 or 1P7.4 containing 5 mM glucose. Erythrocytes were incubated with rotation for 15 h at room temperature; then aliquots of glucose-fed and glucose-deprived erythrocytes (total volume of 200 μL at a 22% hematocrit after additions) were incubated for 2 h at 37 °C in the presence of 5 μM A23187, while others were treated identically after receiving the appropriate volumes of solvent without the ionophore. Each experiment was performed in triplicate.

Effects of Calcium and Calmodulin Antagonist on Erythrocyte Nucleotide Pools. Erythrocytes were prepared from fresh whole blood as described above and resuspended at a 23% hematocrit in 1P7.4 containing 5 mM glucose. Cell suspensions were incubated for 4 h at room temperature with rotation in the presence and absence of the diffusible CaM antagonist, compound 48/80 (750 μg/mL). Aliquots of each cell suspension (total volume of 200 μL at a 22% hematocrit after additions) were then further incubated for 2 h at 37 °C in the presence of 1 μM A23187, 250 μM $CaCl_2$, or both. Controls were treated identically after receiving the appropriate volumes of solvent without additives. Each experiment was performed in triplicate.

Effect of Calmodulin Antagonist on Autoincubated Erythrocyte Nucleotide Pools. Fresh whole blood was collected in ACD (acid, citrate, dextrose) tubes to preserve ATP pools during an overnight incubation at 4 °C in the presence of 10 mg/mL compound 48/80. Preliminary experiments revealed that a higher concentration of CaM antagonist was required to exert an effect on erythrocyte IMP pools during autoincubation, perhaps due to an adsorbing component in the plasma. Controls received an equal volume of water. The next day, whole blood samples were autoincubated (incubated in their own plasma) at 37 °C, and aliquots were removed, processed, and analyzed at 0, 5.5, and 11 h. Each experiment was performed in triplicate on three independent whole blood samples.

Preparation of Acid-Soluble Erythrocyte Extracts and Nucleotide Pool Quantification. Acid-soluble extracts were prepared by adding ice-cold 100% trichloroacetic acid (w/v) to aliquots of erythrocyte or whole blood suspensions [final concentration of 10% (w/v)] and incubating them on ice for 30 min. Extracts were then centrifuged at 14000*g* for 2 min at 4 °C. Supernatants were recovered and neutralized by vortexing for 30 s at room temperature with an equal volume of 0.5 M tri-*N*-octylamine in Freon. Neutralized extracts were then centrifuged at 14000*g* for an additional 2 min, and the upper phase was recovered and stored at −20 °C until further analysis. Nucleotide pools were resolved by anion-exchange chromatography using a previously described protocol (*44*). Briefly, 100 μL of extract was injected onto a Whatman Partisil 10-SAX anion-exchange column and developed with a 40 min linear gradient of 5 mM ammonium dihydrogen phosphate at pH 3.2 (buffer A) and 750 mM ammonium dihydrogen phosphate at pH 4.0 (buffer B) at a flow rate of 2 mL/min. The column eluate was monitored at 254 nm, and peaks were quantified using external standards of known concentration. Metabolite concentrations were normalized to NAD^+ in the extract as previously described (*45*). NAD^+ is a reliable internal standard for these measurements because erythrocyte concentrations of this metabolite are unaffected by autoincubation (*17*).

Effect of Calmodulin and Calmodulin Antagonists on the Association of AMPD Enzymes with Erythrocyte Ghost Membranes. Unsealed erythrocyte ghosts (EG) were prepared from outdated erythrocytes by using the method of Steck and Kant (*46*), as previously described (*12*). In the first set of experiments, increasing concentrations of CaM (0−30 μM) were pretreated for 15 min on ice with 300 μM $CaCl_2$; then approximately 1.5 units of enzyme was added, and the mixtures were incubated for an additional 15 min on ice. Finally, EG (representing 10 μg of protein) suspended in EG binding buffer [5 mM potassium phosphate (pH 7.0), 45 mM potassium chloride, and 0.1 mg/mL bovine serum albumin] were added, and the mixtures were allowed to incubate for an additional 30 min on ice. Partitioning of the AMPD enzyme between the supernatant and pellet was then evaluated by centrifuging the mixture at 14000*g* for 10 min at 4 °C. The supernatant was recovered, and the EG pellet was resuspended in 100 μL of EG binding buffer. EG-bound and unbound AMPD was quantified with an enzyme assay.

In the second set of experiments, increasing concentrations of W13 or the structurally related and 10-fold less potent antagonist, W12, were preincubated with 25 μM Ca^{2+}-CaM for 15 min on ice; then 1.5 units of isoform E was added, and each mixture was incubated for an additional 15 min. Finally, EG were added, and the mixtures were incubated, analyzed, and processed as described above. EG-bound and unbound AMPD was quantified with an enzyme assay.

Enzyme Assay. AMP deaminase activity was measured in 100 μL reaction mixtures containing 25 mM imidazole (pH 7.0), 100 mM potassium chloride, 20 μg of BSA, and 20 mM AMP (unless otherwise stated in the text). The substrate and product were resolved and quantified by anion-exchange HPLC as previously described (*8*, *44*). Kinetic studies were conducted under the assay conditions described above using approximately 40 milliunits of enzyme per assay, variable substrate concentrations (from 0.1 to 24 mM), and initial velocity conditions (product not exceeding 15% of the substrate).

Western Blot Analysis. Proteins were fractionated by 9% SDS−PAGE, electroblotted onto nitrocellulose membranes, and probed with rabbit polyclonal antisera raised against the human AMPD3 recombinant polypeptide, as previously described (*9*, *10*).

Computer-Assisted Statistical Analysis. QuickTTest (version 1.8) developed by S. Ashcroft was used to generate data means and standard deviations and to perform unpaired two-tailed *t*-tests. Paired *t*-tests were performed on the VassarStats Website authored by R. Lowry. Enzfitter was used to calculate kinetic parameters.

RESULTS

Adsorption of AMPD3 Enzymes to Calmodulin−Agarose Beads. Adsorption to CaM−agarose beads has been used previously to demonstrate a protein−protein interaction with Smad proteins (*47*). Figure 1 presents enzyme activity, SDS−PAGE, and Western blot data that demonstrate the adsorption of endogenous and recombinant isoform E to Ca^{2+}-CaM−agarose beads. In addition, this interaction appears to be largely Ca^{2+}-dependent as evidenced by substantially lower affinity for beads that have been pretreated with the calcium chelator, EGTA. The adsorption of isoform E to Ca^{2+}-CaM−agarose beads is also unaffected by physiological changes in pH or ionic strength (data not shown). Figure 2 shows that a series of genetically modified AMPD3 recombinant enzymes truncated up to residue 65 also adsorb to Ca^{2+}-CaM−agarose beads, whereas those lacking 89 and 126 N-terminal residues have substantially reduced affinities for these beads.

Effect of Calmodulin on Isoform E Catalytic Activity. CaM was purified from fresh frozen bovine brain by Phenyl Sepharose chromatography (*43*), treated with EGTA to remove calcium, and extensively dialyzed against water. This purified Ca^{2+}-free preparation was then used to examine the effect of Ca^{2+}-CaM on isoform E catalytic activity. Data presented in Figure 3 and Table 1 reveal that Ca^{2+}-CaM lowers the K_{mapp} of isoform E, whereas Ca^{2+} or CaM alone has no effect on catalytic activity. Consistent with data presented in Figure 2 regarding AMPD3 recombinant enzymes truncated beyond residue 65, Figure 3 also shows that Ca^{2+}-CaM has no measurable effect on the catalytic behavior of

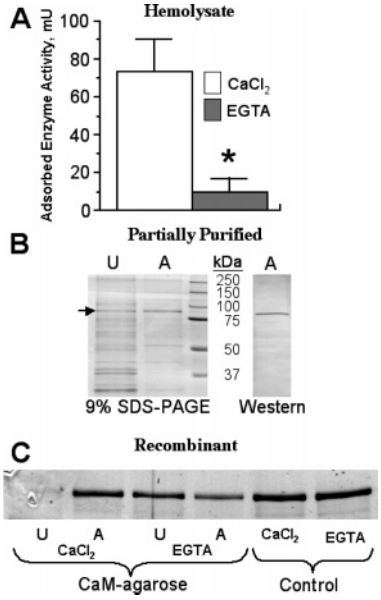

FIGURE 1: Adsorption of isoform E to immobilized Ca^{2+}-calmodulin. (A) Hemolysate isoform E. Fifty microliters of clarified hemolysate was mixed by rotation for 90 min at 4 °C with or without 25 μL of calmodulin immobilized on 4% agarose beads (CaM-bound agarose; 50% slurry) pretreated with 5 mM potassium phosphate (pH 6.6), 45 mM potassium chloride, 0.1% BSA, and either 200 μM $CaCl_2$ or 1 mM EGTA. Mixtures were centrifuged at 14000*g* for 2 min at 4 °C. The supernatants were removed, and the beads were washed several times in the corresponding equilibration buffer ($CaCl_2$ or EGTA) without BSA. Data are presented as adsorbed enzyme activity and represent the mean ± standard deviation of three independent determinations. The asterisk means $p < 0.05$ compared to $CaCl_2$ in a two-tailed *t*-test. (B) Partially purified erythrocyte isoform E. Approximately 1 unit of partially purified erythrocyte isoform E was mixed with Ca^{2+}-CaM−agarose beads using the method described above, except that 0.1% BSA was also omitted from the adsorption buffer. In the left panel is shown 9% SDS−PAGE followed by Coomassie Blue staining of unadsorbed (U) and adsorbed (A) fractions. An arrow points to the 89 kDa isoform E band. Molecular mass standards are labeled. In the right panel is an anti-AMPD3 Western blot of a parallel aliquot of the adsorbed fraction. (C) Recombinant isoform E. Approximately 2 units of enzyme was mixed with Ca^{2+}-CaM−agarose beads using the method described above. Enzyme partitioning was visualized by 9% SDS−PAGE followed by Coomassie Blue staining of unadsorbed (U) and adsorbed (A) fractions. Parallel mixtures without CaM-bound agarose were otherwise treated identically and served as controls.

ΔM90AMPD3, although this enzyme has an inherent greater affinity for substrate than isoform E does (*9*, *11*).

Effects of Glucose Deprivation, the A23187 Ionophore, Calcium Chloride, and Calmodulin Antagonists on Erythrocyte Adenine Nucleotide and IMP Pools. As a means of assessing net changes in ATP catabolism and in vivo flow through the AMPD reaction in response to various conditions of short-term energy imbalance, intracellular adenine nucleotide and IMP pools were quantified in glucose-fed and glucose-starved erythrocytes following a 2 h incubation at 37 °C in the presence or absence of 5 μM A23187. Compared to data for untreated glucose-fed cells, data in Figure 4A show that glucose starvation or exposure to A23187 ionophore alone results in lower levels of ATP and a predominant accumulation of ADP and AMP, but only negligible (≈50%) increases in the size of the IMP pool. Exposing glucose-starved cells to A23187 results in further ATP depletion and additional accumulation of AMP, yet even these higher levels

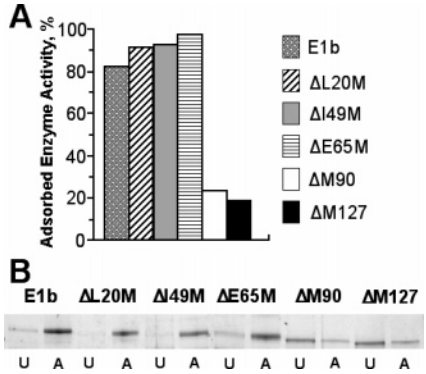

FIGURE 2: Comparative adsorption of human recombinant isoform E and a series of N-truncated AMPD3 enzymes to immobilized Ca^{2+}-calmodulin. Approximately 1 unit of each enzyme was incubated with CaM−agarose beads pretreated with 5 mM potassium phosphate (pH 6.6), 45 mM potassium chloride, 0.1% BSA, and 200 μM $CaCl_2$ using methods and analyses described in the legend of Figure 1: (A) adsorbed enzyme activity and (B) 9% SDS−PAGE followed by Coomassie Blue staining of unadsorbed (U) and adsorbed (A) fractions.

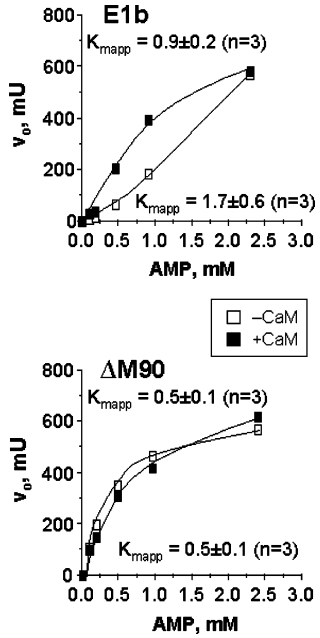

FIGURE 3: Effect of Ca^{2+}-calmodulin on the velocity vs substrate plots of human recombinant isoform E and an N-truncated variant, ΔM90AMPD3. Experiments were performed in the absence of ATP with approximately 40 milliunits of each enzyme per assay under initial velocity (v_o) conditions (product not exceeding 15% of substrate) in the presence (■) and absence (□) of 25 μM Ca^{2+}-CaM. Kinetic parameters were calculated from initial velocities in the presence of increasing substrate concentrations (from 0.09 to 25 mM). The graphs display only those data points for the lowest substrate concentrations from a representative experiment. K_{mapp} values are presented as the means ± standard deviation of three independent determinations.

of substrate do not result in IMP accumulation. Consequently, the total adenine nucleotide pool (∑AMP+ADP+ATP) is preserved under each condition of accelerated erythrocyte ATP catabolism.

Erythrocyte nucleotide pools were also monitored in response to a pathological increase in intracellular Ca^{2+} concentration. Data presented in Figure 4B show that incubation of erythrocytes with a lower concentration of A23187 (1 μM) and $CaCl_2$ (250 μM) results in a significant depletion of ATP that is matched by a near-stoichiometric

Table 1: Ca^{2+}-Calmodulin Activates Isoform E through a K_m Effect

K_{mapp}[a]			
no CaM, no $CaCl_2$	no CaM, 200 μM $CaCl_2$	25 μM CaM, no $CaCl_2$	25 μM CaM, 200 μM $CaCl_2$
1.8 ± 0.1 (n = 4)	1.6 ± 0.3 (n = 3)	1.7 ± 0.2 (n = 3)	1.0 ± 0.1[b] (n = 4)

[a] K_{mapp} values were determined in the absence of ATP and in the presence of 150 mM potassium chloride. [b] $p < 0.05$ when compared to each of the other three conditions in two-tailed t-tests. All other comparisons were not significant.

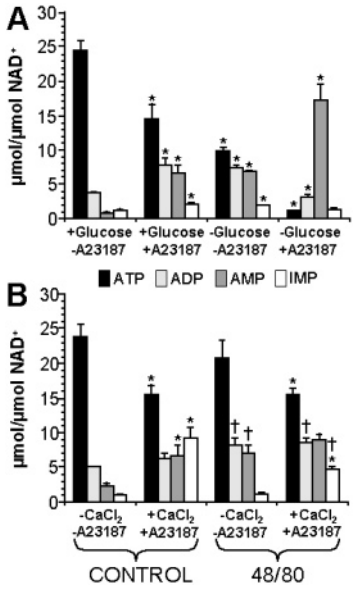

FIGURE 4: Changes in erythrocyte adenine nucleotide and IMP pools in response to short-term energy imbalance. (A) Column graphical representation of acid-soluble nucleotide pools in glucose-fed and glucose-deprived erythrocytes following a 2 h incubation at 37 °C in the presence or absence of 5 μM A23187 ionophore. Data are normalized to the amount of NAD^+ in each extract and represent the mean values ± standard deviation derived from three independent experiments. Asterisks mean $p < 0.05$ when compared to untreated glucose-fed cells in two-tailed t-tests. (B) Column graphical representation of acid-soluble nucleotide pools in untreated (control) and CaM antagonist-treated (750 μg/mL compound 48/80 for 4 h at room temperature) erythrocytes following a 2 h incubation at 37 °C in the presence or absence of 1 μM A23187 and 250 μM $CaCl_2$. Data are normalized to the amount of NAD^+ in each extract and represent the mean values ± standard deviation derived from three independent experiments. Asterisks mean $p < 0.05$ when compared to the absence of ionophore and calcium in unpaired two-tailed t-tests; daggers mean $p < 0.05$ when compared to corresponding control conditions in unpaired two-tailed t-tests.

accumulation of IMP. Conversely, incubation with either A23187 or $CaCl_2$ alone produces no effect on the erythrocyte IMP pool (data not shown). CaM antagonists are structurally diverse compounds that can bind to active Ca^{2+}-CaM complexes, rendering them biologically inert (*48*). Figure 4B also shows that pretreatment with a diffusible CaM antagonist (750 μg/mL compound 48/80 for 4 h at room temperature) significantly slows the Ca^{2+}-induced accumulation of IMP in A23187-treated erythrocytes.

Erythrocyte autoincubation (incubation in their own plasma) reportedly also results in adenine nucleotide catabolism and IMP accumulation during extended periods at 37 °C (*17*). Data presented in Figure 5 confirm these observations and also illustrate that preincubating erythrocytes with compound 48/80 significantly slows the accumulation of IMP under these conditions.

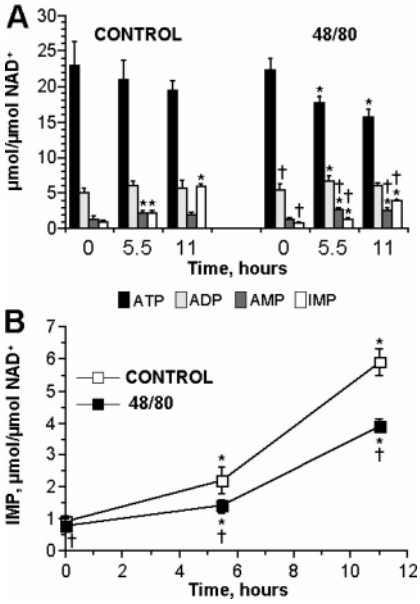

FIGURE 5: Changes in erythrocyte adenine nucleotide and IMP pools during autoincubation at 37 °C. (A) Column graphical representation of acid-soluble nucleotide pools in untreated (control) and compound 48/80-treated (10 mg/mL overnight at 4 °C) erythrocytes during 11 h of autoincubation (incubation in their own plasma). (B) Time course graphical representation of IMP pools during autoincubation. All data are normalized to the amount of NAD^+ in each extract and represent the mean values ± standard deviation derived from three independent experiments (time points in each experiment were analyzed in triplicate). Asterisks mean $p < 0.05$ when compared to the corresponding 0 time in paired two-tailed *t*-tests; daggers mean $p < 0.05$ when compared to the corresponding control time in paired two-tailed *t*-tests.

Effect of Calmodulin on the Association of Isoform E with Erythrocyte Ghost Membranes. Ca^{2+}-CaM antagonizes the membrane association of other proteins (*37*−*39*), and Figure 6 shows that it has a similar effect on the interaction between isoform E and erythrocyte ghost (EG) membranes. This effect becomes significant between 1 and 5 μM Ca^{2+}-CaM and occurs at both neutral (pH 7.0) and acidic (pH 6.5) pH, over a range where isoform E exhibits quantitative differences in its capacity to bind to EG membranes (*12*). Figure 7 demonstrates that a CaM antagonist, W13, disrupts the ability of Ca^{2+}-CaM to interfere with the EG association of isoform E, whereas a 10-fold less potent structural analogue, *N*-(4-aminobutyl)-2-naphthalenesulfonamide (W12), is not as effective. Ca^{2+}-CaM can also displace isoform E from EG membranes, but this requires approximately 10-fold higher effective concentrations (data not shown).

DISCUSSION

AMPD is activated during periods of energy imbalance in most tissues and cells and serves, in part, to maintain the disequilibrium of the adenylate kinase reaction by removing accumulating AMP from the adenylate pool. This effectively minimizes the reduction in adenylate energy charge (*49*) and provides more ATP to the energy-challenged cell through the sustained action of adenylate kinase. Perhaps the most dramatic illustration of this metabolic effect occurs in skeletal muscle where nearly half of the ATP pool can be converted into IMP during sprint exercise (*50*). Following exercise, IMP is predominantly reaminated to AMP, which is then used to rapidly replete the ATP pool (*51*). Conversely, mature

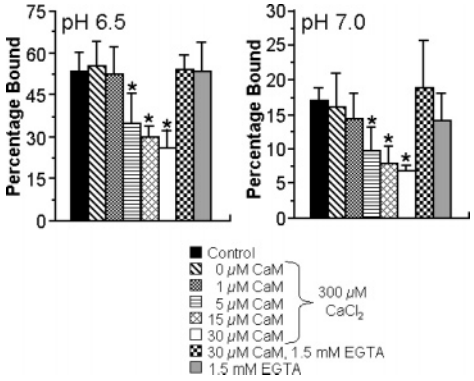

FIGURE 6: Calmodulin antagonizes the association between recombinant isoform E and unsealed erythrocyte ghost membranes. Increasing concentrations of CaM (from 0 to 30 μM) were pretreated for 15 min on ice with 300 μM $CaCl_2$; then approximately 1.5 units of enzyme was added, and the mixtures were incubated for an additional 15 min on ice. Finally, EG (10 μg of protein) were added, and the mixtures were allowed to incubate for an additional 30 min on ice. Partitioning was accomplished by centrifugation at 14000*g* for 10 min at 4 °C. Parallel mixtures, including a no addition control and those pretreated with 1.5 mM EGTA with (30 μM) or without CaM, were treated identically. Data are presented as the percentage of enzyme activity bound to EG and represent the mean ± standard deviation of four independent experiments. Asterisks mean $p < 0.05$ when compared to control. All other differences were not statistically significant.

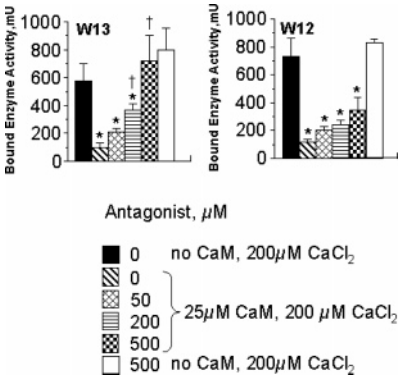

FIGURE 7: Antagonists reverse the effect of calmodulin on the association between recombinant isoform E and unsealed erythrocyte ghost membranes. Increasing concentrations (from 0 to 500 μM) of the calmodulin antagonists, W13 (left graph and panel) and W12 (right graph and panel), were preincubated with 25 μM CaM and 200 μM $CaCl_2$ for 15 min on ice, and then approximately 1 unit of enzyme was added to each mixture for incubation for an additional 15 min on ice. Finally, erythrocyte ghosts (10 μg of protein) were added and the mixtures incubated for an additional 30 min on ice. Partitioning and analyses were then performed as described in the legend of Figure 6. Parallel mixtures without CaM, but containing 200 μM $CaCl_2$ alone or in combination with 500 μM antagonist, were treated identically and served as controls. In the graphs, data represent the mean ± standard deviation of three independent experiments. Asterisks mean $p < 0.05$ when compared to either no CaM control in a two-tailed *t*-test; daggers mean $p < 0.05$ when compared to the identical W12 concentration in a two-tailed *t*-test.

erythrocytes are unable to synthesize ATP from IMP due to a developmental loss of adenylosuccinate synthetase (*13*, *14*), an integral component of the only known metabolic pathway in mammalian cells able to aminate position 6 of the hypoxanthine ring structure. Alternatively, these cells do retain the necessary enzymatic machinery for synthesizing ATP from the salvageable purine catabolites, adenosine and adenine, but the circulating levels of these compounds are

quite low under steady-state conditions, i.e., <1 μM (*52*, *53*). Consequently, mature erythrocytes may be uniquely susceptible to irreversible adenine nucleotide depletion by AMP deamination, particularly under conditions where isoform E is activated.

However, mature erythrocytes seem to be equipped to effectively minimize the potentially deleterious consequences of AMP deamination under several experimental conditions of short-term energy imbalance. For example, AMP rather than IMP accumulates during periods of accelerated ATP turnover in response to glucose deprivation or during incubation with A23187 alone (refs *22* and *54* and this study). These observations appear to reflect potent isoform E inhibition that may be a protective mechanism for prolonging erythrocyte survival. The basis for isoform E inhibition was not addressed in this study, but is likely related to high erythrocytic levels of identified competitive inhibitors, 2,3-DPG and Pi (*55*, *56*), or to intracellular membrane association where this enzyme can interact with the potent noncompetitive inhibitor, PtdIns(4,5)P2 (*10*, *12*).

Ca^{2+} has been proposed as an antagonist of an AMPD inhibitor in erythrocytes that is weakened in its action by dilution or lost during purification (*23*). Data presented in this study provide a potential mechanism for explaining these observations by demonstrating that Ca^{2+} acts indirectly to activate erythrocyte AMPD through a protein−protein interaction between Ca^{2+}-calmodulin (Ca^{2+}-CaM) and isoform E. Ca^{2+}-CaM promotes greater isoform E catalytic activity in the presence of physiological concentrations of substrate by (1) direct activation through a K_{mapp} effect, similar to the effect Ca^{2+} has on erythrocyte hemolysate AMPD (*23*), and (2) antagonism of cytoplasmic membrane binding, thus preventing the catalytic inhibition that is associated with this protein−lipid interaction (*12*). Notably, the protein−protein interaction with Ca^{2+}-CaM can overcome isoform E inhibition during periods of short-term erythrocyte energy imbalance that are accompanied by a pathological increase in intracellular Ca^{2+} concentration or during extended autoincubation at 37 °C in the presence of physiological concentrations of this divalent cation. This regulatory mechanism was demonstrated in this study by the inhibited accumulation of IMP when erythrocytes were preincubated with a CaM antagonist and then exposed to either of these conditions.

Consequently, Ca^{2+}-CaM activation of isoform E can be predicted to result in pathophysiological consequences in mature erythrocytes. For example, this regulatory mechanism may contribute to the metabolic imbalance that promotes accelerated hemolysis of circulating erythrocytes in familial phosphofructokinase deficiency (Tarui's disease; glycogen storage disease type VII). Reported indicators of a disturbed erythrocyte energy balance in these patients are consistent with this hypothesis, such as elevated intracellular calcium concentrations (*57*), 14−23% smaller total adenine nucleotide pools (*17*, *58*), and 16-fold higher levels of IMP (*17*). Patient erythrocytes also exhibit accelerated rates of adenine nucleotide depletion and IMP accumulation during periods of experimental autoincubation (*17*). Consequently, Ca^{2+}-CaM activation of isoform E should be considered to contribute to erythrocyte manifestations of familial phosphofructokinase deficiency, as well as other pathophysiological situations of energy imbalance associated with increased calcium concentrations, such as sickle-cell erythrocytes (reviewed in ref *59*) and Alzheimer's disease brain (*60*, *61*).

Specific effects on isoform E behavior shown to occur in vitro are observed with physiological concentrations of Ca^{2+}-CaM, which are between 2 and 26 μM in the soluble fraction of mammalian tissues and cells, while up to 50% more can be found in the particulate fraction (*36*). Consequently, the protein−protein interaction between Ca^{2+}-CaM and isoform E may contribute to purine nucleotide catabolic regulation in other tissues and cells that express the AMPD3 gene. However, the metabolic consequence of this association may be different because of the capacity for IMP reamination to AMP. In addition, most human tissues and cells express more than one AMPD gene and can produce a large array of AMPD tetrameric enzymes comprised of mixed isoform-specific subunits (*40*, *41*). Consequently, an evaluation of purified mixed tetrameric AMPD3 subunit-containing enzymes as potential targets for Ca^{2+}-CaM seems to be warranted. In addition, metabolic experiments similar to those conducted in this study should be performed in cells where AMPD3 and other gene family members are coexpressed.

The combined results of this study allow us to refine our model for isoform E regulation in mature erythrocytes (*12*). As illustrated in Figure 8, isoform E can be effectively maintained in an inactive T state by a combination of soluble small molecule effectors and a protein−lipid interaction with the cytoplasmic membrane. P_i and 2,3-DPG are present in millimolar concentrations in mature erythrocytes (*62*), whereas the protein−lipid interaction is sensitive to physiological changes in pH due to an ionic attraction between exposed histidine residues in isoform E and negative charges on the cytoplasmic face of the membrane bilayer (*12*). The identity of the anionic membrane moiety is proposed to be phosphate headgroups of phosphatidylinositol 4,5-bisphosphate (PtdIns-[4,5]P2), a potent noncompetitive inhibitor of isoform E (*10*). Accordingly, the proportion of isoform E enzymes partitioning into the particulate fraction is proposed to increase during periods of metabolic acidosis, such as rapid ATP catabolism. Mature erythrocytes may use any or all of these inhibitory mechanisms to keep isoform E in the T state during short periods of energy imbalance, which leads to an accumulation of AMP, rather than IMP. The protein−protein interaction with Ca^{2+}-CaM provides a counter-regulatory mechanism by directly activating isoform E and antagonizing the cytoplasmic membrane association of this enzyme. These combined effects convert isoform E into the R state and shift adenine nucleotide catabolic flow toward the production of IMP, which results in an irreversible depletion of the erythrocyte adenine nucleotide pool.

Finally, relative adsorption to Ca^{2+}-CaM−agarose beads across a series of N-truncated recombinant enzymes identifies potential binding determinants within residues 65−89 of the AMPD3 polypeptide. These data add to a growing list of observations that together underscore the significance of divergent N-terminal sequence in isoform E. Moreover, enzyme behaviors that were shown in this study to be affected by the interaction with Ca^{2+}-CaM have previously been related to N-terminal sequence. For example, up to 48 N-terminal amino acids are involved in suppressing contractile protein binding (*11*) and pH-resistant membrane interactions (*12*). These combined effects may permit isoform E to interact reversibly with membranes in response to

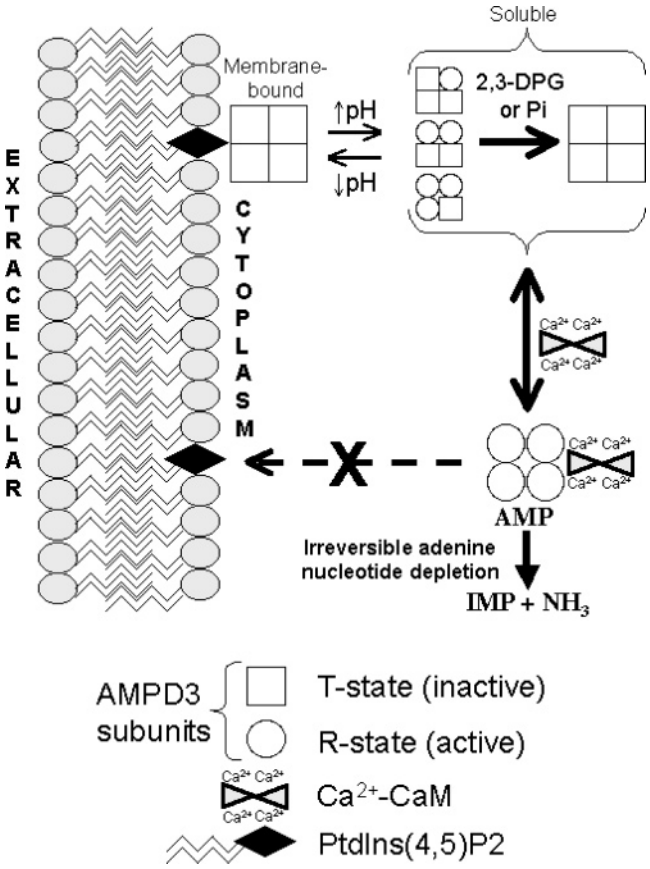

FIGURE 8: Model for erythrocyte isoform E regulation. Small molecule effectors and macromolecular interactions can modulate catalytic activity and affect the catabolic flow through the AMP branch point. Competitive inhibition of isoform E catalytic activity is exerted by P_i and 2,3-DPG and noncompetitive inhibition by PtdIns(4,5)P2, with the latter involving pH-dependent recruitment to the cytoplasmic membrane. Isoform E inhibition causes AMP to accumulate during short periods of energy imbalance, which can ultimately shift the catabolic flow through cytosolic 5′-nucleotidase I with a resulting production of adenosine. Binding of Ca^{2+}-CaM to isoform E overcomes these inhibitory mechanisms by directly activating isoform E and antagonizing the membrane association of this enzyme. This protein−protein interaction is reversible and likely controlled by intracellular concentrations of Ca^{2+}. Isoform E activation diverts the catabolic flow through the AMPD reaction and produces IMP. This irreversibly depletes the adenine nucleotide pool, because mature erythrocytes are unable to convert IMP back to AMP.

physiological changes in pH in skeletal muscle, where the relative level of AMPD3 gene expression is greatest (*7*). Although it is not known how these suppressive effects are structurally related, both more strongly affect C-terminal amino acids in the AMPD3 polypeptide, i.e., putative contractile protein binding determinants that reside within residues 192−347 (*11*) and positive charges other than protonated histidine residues located to the C-terminal side of residue 126 (*12*), respectively. Ca^{2+}-CaM antagonizes the membrane association of isoform E without affecting the pH responsiveness of this protein−lipid interaction. In addition, up to 89 N-terminal amino acids appear to play a role in catalytic autoinhibition of isoform E [K_{mapp}, 1.7 ± 0.6 mM vs 0.5 ± 0.1 mM for ΔM90AMPD3, $p < 0.05$ in a two-tailed *t*-test ($n = 3$); see Figure 4]. Ca^{2+}-CaM alters this behavior by significantly increasing substrate affinity. These combined observations provide a rationale for planned structural studies for identifying Ca^{2+}-CaM binding determinants in the N-terminal sequence of the human AMPD3 polypeptide and for defining how this association alters the functional conformation of isoform E.

ACKNOWLEDGMENT

The authors thank the staff of Occupational Health Services at the Medical College of Wisconsin for drawing fresh blood used in this study.

REFERENCES

1. Sommerschild, H. T., and Kirkboen, K. A. (2000) Adenosine and cardioprotection during ischaemia and reperfusion: An overview, *Acta Anaesthesiol. Scand. 44*, 1038−1055.
2. Dunwiddie, T. V., and Masino, S. A. (2001) The role and regulation of adenosine in the central nervous system, *Annu. Rev. Neurosci. 24*, 31−55.
3. Linden, J. (2001) Molecular approach to adenosine receptors: Receptor-mediated mechanisms of tissue protection, *Annu. Rev. Pharmacol. Toxicol. 41*, 775−787.
4. Sabina, R. L., Morisaki, T., Clarke, P., Eddy, R., Shows, T. B., Morton, C. C., and Holmes, E. W. (1990) Characterization of the human and rat myoadenylate deaminase genes, *J. Biol. Chem. 265*, 9423−9433.
5. Mahnke-Zizelman, D. K., Van den Bergh, F., Bausch-Jurken, M. T., Eddy, R., Sait, S., Shows, T. B., and Sabina, R. L. (1996) Cloning, sequence and characterization of the human *AMPD2* gene: Evidence for transcriptional regulation by two closely spaced promoters, *Biochim. Biophys. Acta 1308*, 122−132.
6. Mahnke-Zizelman, D. K., Eddy, R., Shows, T. B., and Sabina, R. L. (1996) Characterization of the human *AMPD3* gene reveals that 5′ exon useage is subject to transcriptional control by three tandem promoters and alternative splicing, *Biochim. Biophys. Acta 1306*, 75−92.
7. Mahnke-Zizelman, D. K., and Sabina, R. L. (1992) Cloning of human AMP deaminase isoform E cDNAs: Evidence for a third *AMPD* gene exhibiting alternatively spliced 5′-exons, *J. Biol. Chem. 267*, 20866−20877.
8. Bausch-Jurken, M. T., Mahnke-Zizelman, D. K., Morisaki, T., and Sabina, R. L. (1992) Molecular cloning of AMP deaminase isoform L: Sequence and bacterial expression of human AMPD2 cDNA, *J. Biol. Chem. 267*, 22407−22413.
9. Mahnke-Zizelman, D. K., Tullson, P. C., and Sabina, R. L. (1998) Novel aspects of tetramer assembly and function are revealed by recombinant expression of human AMP deaminase isoforms, *J. Biol. Chem. 273*, 35118−35125.
10. Sims, B., Mahnke-Zizelman, D. K., Profit, A. A., Prestwich, G. D., Sabina, R. L., and Theibert, A. B. (1999) Regulation of AMP deaminase by phosphoinositides, *J. Biol. Chem. 274*, 25701−25707.
11. Mahnke-Zizelman, D. K., and Sabina, R. L. (2001) Localization of N-terminal sequences in human AMP deaminase isoforms that influence contractile protein binding, *Biochem. Biophys. Res. Commun. 285*, 489−495.
12. Mahnke-Zizelman, D. K., and Sabina, R. L. (2002) N-Terminal sequence and distal histidine residues are responsible for pH-regulated cytoplasmic membrane binding of human AMP deaminase isoform E, *J. Biol. Chem. 277*, 42654−42662.
13. Bishop, C. (1960) Purine metabolism in human and chicken blood, *in vitro*, *J. Biol. Chem. 235*, 3228−3232.
14. Lowy, B. A., and Dorfman, B.-Z. (1970) Adenylosuccinase activity in human and rabbit erythrocyte lysates, *J. Biol. Chem. 245*, 3043−3046.
15. Tavazzi, B., Di Pierro, D., Amorini, A. M., Fazzina, G., Tuttobene, M., Giardina, B., and Lazzarino, G. (2000) Energy metabolism and lipid peroxidation of human erythrocytes as a function of increased oxidative stress, *Eur. J. Biochem. 267*, 684−689.
16. Tavazzi, B., Amorini, A. M., Fazzina, G., Di Pierro, D., Tuttobene, M., Giardina, B., and Lazzarino, G. (2001) Oxidative stress induces impairment of human erythrocyte energy metabolism through the oxygen radical-mediated direct activation of AMP-deaminase, *J. Biol. Chem. 276*, 48083−48092.
17. Ronquist, G., Rudolph, O., Engstrom, I., and Waldenstrom, A. (2001) Familial phosphofructokinase deficiency is associated with a disturbed calcium homeostasis, *J. Intern. Med. 249*, 85−95.

18. Ogasawara, N., Goto, H., Yamada, Y., Nishigaki, I., Itoh, T., and Hasegawa, I. (1984) Complete deficiency of AMP deaminase in human erythrocytes, *Biochem. Biophys. Res. Commun. 122*, 1344−1349.
19. Yamada, Y., Goto, H., Murase, T., and Ogasawara, N. (1994) Molecular basis for human erythrocyte AMP deaminase deficiency: Screening for the major point mutation and identification of other mutation, *Hum. Mol. Genet. 3*, 2243−2245.
20. Yamada, Y., Makarewicz, W., Goto, H., Nomura, N., Kitoh, H., and Ogasawara, N. (1998) Gene mutations responsible for human erythrocyte AMP deaminase deficiency in poles, *Adv. Exp. Med. Biol. 431*, 347−350.
21. Almarez, L., Garcia-Sancho, J., and Lew, V. L. (1988) Calcium-induced conversion of adenine nucleotides to inosine monophosphate in human red cells, *J. Physiol. 407*, 557−567.
22. Engstrom, I., Waldenstrom, A., and Ronquist, G. (1996) Activation of AMP deaminase in human erythrocytes by calcium ions, *Scand. J. Clin. Lab. Invest. 56*, 345−350.
23. Almarez, L., and Garcia-Sancho, J. (1989) Activation by calcium of AMP deaminase from the human red cell, *FEBS Lett. 244*, 417−420.
24. Askari, A. (1963) Erythrocytes: 5′-Adenylic acid deaminase requirement for ammonia or monovalent cation, *Science 141*, 44−45.
25. Sims, B., Powers, R. E., Sabina, R. L., and Theibert, A. B. (1998) Elevated adenosine monophosphate deaminase activity in Alzheimer's disease brain, *Neurobiol. Aging 19*, 385−391
26. Hohl, A. M., and Hohl, C. M. (1999) Isolation and regulation of piglet cardiac AMP deaminase, *Mol. Cell. Biochem. 201*, 151−158.
27. Wozniak, M., Kossowska, E., Purzycka-Preis, J., and Zydowo, M. M. (1988) The influence of phosphatidate bilayers on pig heart AMP deaminase, *Biochem. J. 255*, 977−981.
28. Tanfani, F., Kossowska, E., Purzycka-Preis, J., Zydowo, M. M., Wozniak, M., Tartaglini, E., and Bertoli, E. (1993) The interaction of phospholipid bilayers with pig heart AMP deaminase: Fourier-transform infrared spectroscopic and kinetic studies, *Biochem. J. 291*, 921−926.
29. Tanfani, F., Kulawiak, D., Kossowska, E., Purzycka-Preis, J., Zydowo, M. M., Sarkissova, E., Bertoli, E., and Wozniak, M. (1998) Structural-functional relationships in pig heart AMP-deaminase in the presence of ATP, orthophosphate, and phosphatidate bilayers, *Mol. Gen. Metab. 65*, 51−58.
30. Pipoly, G. M., Nathans, G. R., Chang, D., and Deuel, T. F. (1979) Regulation of the interaction of purified human erythrocyte AMP deaminase and the human erythrocyte membrane, *J. Clin. Invest. 63*, 1066−1076.
31. Ranieri-Raggi, M., and Raggi, A. (1980) Effects of storage on activity and subunit structure of rabbit skeletal-muscle AMP deaminase, *Biochem. J. 189*, 367−368.
32. Marquetant, R., Sabina, R. L., and Holmes, E. W. (1989) Identification of a noncatalytic domain in AMP deaminase that influences binding to myosin, *Biochemistry 28*, 8744−8749.
33. Chilson, O. P., Kelly-Chilson, A. E., and Siegel, N. R. (1997) AMP-deaminases from chicken and rabbit muscle: Partial primary sequences of homologous 17-kDa CNBr fragments: Autorecognition by rabbit anti-[chicken AMPD], *Comp. Biochem. Physiol. 116B*, 371−377.
34. Knecht, K., Wiesmuller, K.-H., Gnau, V., Jung, G., Meyermann, R., Todd, K. G., and Hamprecht, B. (2001) AMP deaminase in rat brain: Localization in neurons and ependymal cells, *J. Neurosci. Res. 66*, 941−950.
35. Chin, D., and Means, A. R. (2000) Calmodulin: A prototypical calcium sensor, *Trends Cell Biol. 10*, 322−328.
36. Kakiuchi, S., Yasuda, S., Yamazaki, R., Teshima, Y., Kanda, K., Kakiuchi, R., and Sobue, K. (1982) Quantitative determinations of calmodulin in the supernatant and particulate fractions of mammalian tissues, *J. Biochem. 92*, 1041−1048.
37. Kim, J., Shishido, T., Jiang, X., Aderem, A., and McLaughlin, S. (1994) Phosphorylation, high ionic strength, and calmodulin reverse the binding of MARCKS to phospholipid vesicles, *J. Biol. Chem. 269*, 28214−28219.
38. Park, J. B., Farnsworth, C. C., and Glomset, J. A. (1997) Ca^{2+}/calmodulin causes Rab3A to dissociate from synaptic membranes, *J. Biol. Chem. 272*, 20857−20865.
39. Dell'Acqua, M. L., Faux, M. C., Thorburn, J., Thorburn, A., and Scott, J. D. (1998) Membrane-targeting sequences on AKAP79 bind phosphatidylinositol-4,5-bisphosphate, *EMBO J. 17*, 2246−2260.
40. Ogasawara, N., Goto, H., Yamada, Y., Watanabe, T., and Asano, T. (1982) AMP deaminase isozymes in human tissues, *Biochim. Biophys. Acta 714*, 298−306.
41. Ogasawara, N., Goto, H., Yamada, Y., and Watanabe, T. (1984) Distribution of AMP deaminase isozymes in various human blood cells, *Int. J. Biochem. 16*, 269−273.
42. Nathans, G. R., Chang, D., and Deuel, T. F. (1978) AMP deaminase from human erythrocytes, *Methods Enzymol. 51*, 497−502.
43. Gopalakrishna, R., and Anderson, W. B. (1982) Ca^{2+}-induced hydrophobic site on calmodulin: Application for purification of calmodulin by phenyl-sepharose affinity chromatography, *Biochem. Biophys. Res. Commun. 104*, 830−836.
44. Swain, J. L., Sabina, R. L., McHale, P. A., Greenfield, J. C., and Holmes, E. W. (1982) Prolonged myocardial nucleotide depletion after brief ischemia in the open-chest dog, *Am. J. Physiol. 242*, H818−H826.
45. Sabina, R. L., Swain, J. L., Bradley, W. G., and Holmes, E. W. (1984) Quantitation of metabolites in human skeletal muscle during rest and exercise: A comparison of methods, *Muscle Nerve 7*, 77−82.
46. Steck, T. L., and Kant, J. A. (1974) Preparation of impermeable ghosts and inside out vesicles from human erythrocyte membranes, *Methods Enzymol. 31*, 172−180.
47. Zimmerman, C. M., Kariapper, M. S. T., and Mathews, L. S. (1998) Smad proteins physically interact with calmodulin, *J. Biol. Chem. 273*, 677−680.
48. Beitner, R. (1998) Calmodulin antagonists and cell energy metabolism in health and disease, *Mol. Genet. Metab. 64*, 161−168.
49. Chapman, A. G., and Atkinson, D. E. (1973) Stabilization of adenylate energy charge by the adenylate deaminase reaction, *J. Biol. Chem. 248*, 8309−8312.
50. Norman, B., Sabina, R. L., and Jansson, E. (2001) Regulation of skeletal muscle ATP catabolism by AMPD1 genotype during sprint exercise in asymptomatic subjects, *J. Appl. Physiol. 91*, 258−264.
51. Sahlin, K., Palmskog, G., and Hultman, E. (1978) Adenine nucleotide and IMP contents of the quadriceps muscle in man after exercise, *Pfluegers Arch. 374*, 193−198.
52. Moser, G. H., Schrader, J., and Deussen, A. (1989) Turnover of adenosine in plasma of human and dog blood, *Am. J. Physiol. 256*, C799−C806.
53. Ericson, A., Groth, T., Niklasson, F., and De Verdier, C. H. (1980) Plasma concentration and renal excretion of adenine and 2,8-dihydroxyadenine after administration of adenine in man, *Scand. J. Clin. Invest. 40*, 1−8.
54. Engstrom, I., Waldenstrom, A., and Ronquist, G. (1993) Ionophore A23187 reduces energy charge by enhanced calcium ion pumping in suspended human erythrocytes, *Scand. J. Clin. Lab. Invest. 53*, 239−246.
55. Lian, C.-Y., and Harkness, D. R. (1974) The kinetic properties of adenylate deaminase from human erythrocytes, *Biochim. Biophys. Acta 341*, 27−40.
56. Yun, S.-Y., and Suelter, C. H. (1978) Human erythrocyte 5′-AMP aminohydrolase: Purification and characterization, *J. Biol. Chem. 253*, 404−408.
57. Waldenstrom, A., Engstrom, I., and Ronquist, G. (2001) Increased erythrocyte content of Ca^{2+} in patients with Tarui's disease, *J. Int. Med. 249*, 97−102.
58. Shimizu, T., Kono, N., Kiyokawa, H., Yamada, Y., Hara, N., Mineo, I., Kawachi, M., Nakajima, H., Wang, Y. L., and Tarui, S. (1988) Erythrocyte glycolysis and its marked alteration by muscular exercise in Type VII glycogenosis, *Blood 71*, 1130−1134.
59. Dover, G. J., and Platt, O. S. (1998) Sickle cell disease, in *Hematology in Infancy & Childhood* (Nathan, D. G., and Orkin, S. H., Eds.) W. B. Saunders, Philadelphia.
60. La Ferla, F. M. (2003) Calcium dyshomeostasis and intracellular signaling in Alzheimer's disease, *Nat. Rev. 3*, 862−872.
61. O'Day, D. H., and Myre, M. A. (2004) Calmodulin-binding domains in Alzheimer's disease proteins: Extending the calcium hypothesis, *Biochem. Biophys. Res. Commun. 320*, 1051−1054.
62. Bontemps, F., Van den Berghe, G., and Hers, H. G. (1986) Pathways of adenine nucleotide catabolism in erythrocytes, *J. Clin. Invest. 77*, 824−830.

BI048121P